Neurospine 2020;17(1):42-59.
https://doi.org/10.14245/ns.2040052.026

Neurospine
pISSN 2586-6583 eISSN 2586-6591

Original Article

Corresponding Author
Marianna Peroglio
https://orcid.org/0000-0002-5458-3446

AO Research Institute Davos,
Clavadelerstrasse 8, 7270 Davos,
Switzerland
E-mail: marianna.peroglio@aofoundation.org

Received: January 31, 2020
Revised: February 27, 2020
Accepted: February 28, 2020

Direct and Intervertebral Disc-Mediated Sensitization of Dorsal Root Ganglion Neurons by Hypoxia and Low pH

Junxuan Ma, Despina Stefanoska, Sibylle Grad, Mauro Alini, Marianna Peroglio

AO Research Institute Davos, Davos, Switzerland

Objective: Ischemia-related risk factors are consistently correlated with discogenic pain, but it remains unclear how the ischemia-associated hypoxia and acidosis influence the peripheral sensory nervous system, namely the dorsal root ganglion (DRG), either directly or indirectly via intervertebral disc (IVD) mediation.
Methods: Bovine tail IVD organ cultures were preconditioned in different hypoxic and/or acidic conditions for 3 days to collect the conditioned medium (CM). The DRG-derived ND7/23 cells were either treated by the IVD CM or directly stimulated by hypoxic and/or acidic conditions. Neuronal sensitization was evaluated using calcium imaging (Fluo-4) after 3 days.
Results: We found that direct exposure of DRG cell line to hypoxia and acidosis increased both spontaneous and bradykinin-stimulated calcium response compared to normoxia-neutral pH cultures. Hypoxia and low pH in combination showed stronger effect than either parameter on its own. Indirect exposure of DRG to hypoxia-acidosis-stressed IVD CM also increased spontaneous and bradykinin-stimulated response, but to a lower extent than direct exposure. The impact of direct hypoxia and acidosis on DRG was validated in a primary sheep DRG cell culture, showing the same trend.
Conclusion: Our data suggest that targeting hypoxia and acidosis stresses both in IVD and DRG could be a relevant objective in discogenic pain treatment.

Keywords: Low back pain, Intervertebral disc, Dorsal root ganglion, Calcium Imaging, Hypoxia, Acidosis

INTRODUCTION

Low back pain (LBP) represents a major health problem owing to its frequency and consequences on professional life.[1] Intervertebral disc degeneration is commonly associated with back pain.[2,3] Despite its multifactorial nature, ischemia-related risk factors (aortic calcification, stenosis of lumbar arteries, smoking and high serum cholesterol levels) are consistently correlated with discogenic pain.[4-6]

Nutrient supply in the avascular IVD is highly dependent on endplate diffusion.[7] As a result of ischemia, the oxygen concentration in the IVD can decrease to a level below the metabolic requirements. Reduction in oxygen delivery below tissue demand is defined as hypoxia.[8] Moreover, local low pH decreases due to the accumulation of lactate under hypoxic metabolism and failed circulation transport due to ischemia. Bio-markers of hypoxia such as hypoxia-inducible factor 1-alpha, glucose transporter type 1, 3, and 9 were upregulated in the degenerative IVD,[9,10] while high lactate concentrations associated with anaerobic metabolism were found in the IVD associated with discogenic pain.[11] Electrode measurements of the IVD during surgery found that the pH varied with the degree of degeneration and could fall below 6.0.[12]

It is known that the dorsal root ganglion (DRG) contains the cell bodies of the primary sensory neurons responsible for transducing and modulating sensory signals including nociception and/or pain.[13] The pathological discharge of the DRG neurons transmits noxious or painful information to the central sensory

nervous system (CNS) and is believed to be one biological basis of pain.[14,15] Experiments in animal models proved that spontaneous unprovoked pain, paresthesias, dysthesias, pain evoked by normally innocuous stimuli (allodynia) and exaggerated pain due to noxious stimuli (hyperalgesia), which are all typically associated with chronic pain symptom,[16] largely depend on the peripheral input from DRG neurons.[17,18]

Former studies showed that the inflammatory, degenerative IVD can cause an increase in the endoneural fluid pressure[19,20] leading to the ischemia of the DRG.[21-24] Hence, the ischemia-associated factors, namely hypoxia and acidosis, may directly influence DRG.[25-27] The direct exposure of DRG to hypoxia and acidosis was defined as 'direct effect.' Alternatively, hypoxia- and acidosis-stressed IVD may release molecules that influence DRG sensitization.[27] We defined this IVD-mediated effect as 'indirect effect.' Our hypothesis is that both 'direct effect' and 'indirect effect' of hypoxia and low pH can lead to DRG neuron neuropathy with spontaneous discharge or discharge evoked by bradykinin.

In this context, *in vitro* models are useful for studying pain-related neural physiology. In this study, the DRG-derived ND7/23 cell line was used. It is derived from cell fusion of N18Tg2 mouse neuroblastoma and neonatal rats DRG neurons.[28] This cell line has been chosen since after differentiation, the ND7/23 cells display sensory neuron-like properties, such as depolarization in response to bradykinin and capsaicin and expression of neuropeptide substance P.[28] To ensure translational relevance of the study, primary DRG cells harvested from adult sheep were used to validate key findings obtained with the cell line.

Calcium imaging is a powerful tool to evaluate intracellular calcium signal within a large population of peripheral sensory neurons and to study pain mechanisms.[29,30] The transient increase of intracellular calcium levels following neuronal discharge is a key step for neurotransmitter release which is both enough and necessary for the synaptic transmission of nociceptive (pain) signal to the CNS.[31] Furthermore, former studies comparing calcium imaging with electrophysiological measurement using patch clamp showed that increases in intracellular calcium level detected using calcium imaging reliably and, within a certain range, linearly reflect neuronal firing. Additionally, patterns of action potentials in individual cells can be deduced from calcium recordings.[32-34]

In this study, DRG cells were either directly exposed to hypoxia and acidosis, or indirectly (The indirect effect was evaluated by stimulating the DRG cells with hypoxia and acidosis treated IVD conditioned medium [CM], where hypoxia and acidosis were not directly applied to DRG.). The effect of hypoxia alone, acidosis alone or their combination were investigated. Spontaneous and bradykinin-stimulated response of DRG cells was evaluated using calcium imaging of both soma (cell body) and neurite outgrowth. Key output parameters included calcium peak frequency, peak height, and proportion of cells responding to bradykinin.

MATERIALS AND METHODS

The study design included: (1) Direct influence of hypoxia and acidosis on DRG sensitization (Fig. 1A); (2) Indirect influence of hypoxia and acidosis: influence of hypoxia-acidosis-stressed IVD on DRG sensitization. Hypoxia and/ or acidosis were applied to IVDs for 3 days. Following this preconditioning, IVDs were cultured in normoxia and neutral pH for collection of IVD CM used to stimulate DRG cells (Fig. 1B).

1. ND7/23 Cell Line Culture and Neural Differentiation

DRG neuron-derived ND7/23 cells (Sigma-Aldrich, St. Louis, MI, USA; cat. no. 92090903) were expanded in 4.5-g/L glucose Dulbecco's Modified Eagle Medium (DMEM; Gibco, Paisley, UK; cat. no. 52100-021), 10% fetal calf serum (FCS; Sera Plus, Biotech, Aidenbach, Germany; cat. no. 3702-P121812), 1% penicillin/streptomycin (P/S, cat. no. 15140-122; Gibco), and 0.11-g/L sodium pyruvate (cat. no. P5280; Sigma-Aldrich). The cells were cultured at 37°C and 5% CO_2 and passaged every 4 days. Passage 8 ND7/23 cells were used for the study, while cell seeding density was 10,000 cells/cm^2 for both routine passage and the study designs.

Since neural differentiation is necessary to achieve electrophysiological properties similar to those observed in primary sensory neurons in culture, neural differentiation was induced by adding 1 mM N6,2′-O-Dibutyryladenosine 3′,5′-cyclic monophosphate sodium salt (cAMP, Sigma-Aldrich; cat. no. D0260) and 10-ng/mL recombinant rat beta-nerve growth factor (NGF; R&D Systems Inc., Minneapolis, MN; US; cat. no. 556-NG-100)[28,35] to either IVD CM (supplemented with 0.5% FCS) or DMEM (supplemented with 1% penicillin/streptomycin and 0.11-g/L sodium pyruvate) 1 hour after cell seeding.

2. Direct Exposure of ND7/23 Cells to Different Combinations of pH and Oxygen Level

ND7/23 cells were seeded in 48-well plates at a density of 10,000 cells/cm^2. After 1h of cell attachment in standard culture conditions (pH 7.4, O_2 20%, cultured in DMEM with 0.11-g/L sodium pyruvate, 10% FCS and 1% P/S), the culture medium

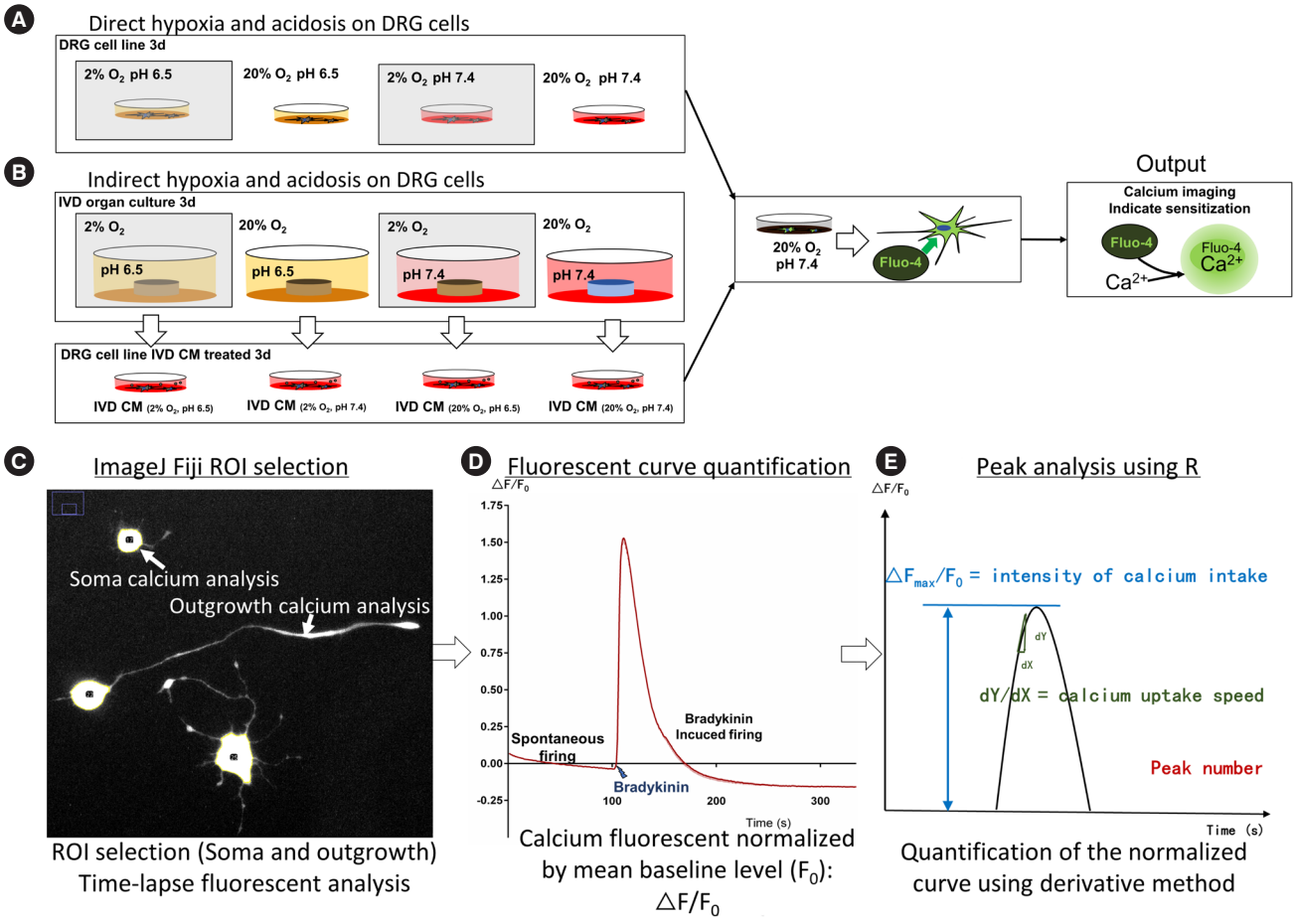

Fig. 1. Experimental setting of ND7/23 cells stimulated either directly by hypoxia and/or low pH stress (A) or indirectly by the conditioned medium from bovine IVDs preconditioned by hypoxia and/or low pH (B). (C-E) Workflow of calcium imaging data analysis. DRG, dorsal root ganglion; IVD, intervertebral disc; CM, conditioned medium; ROI, region of interest.

was replaced by neural differentiation medium adjusted at different pHs and/or different oxygen tensions (pH 7.4, O_2 20%; pH 6.5, O_2 20%; pH 7.4, O_2 2%; and pH 6.5, O_2 2%). Hypoxia condition was created by setting the oxygen level at 2% in the low oxygen incubator (Thermo Fisher Scientific, Waltham, MA, USA), while normoxia culture was maintained in a standard tissue culture incubator at 20% oxygen (5% CO_2 in both conditions). The pH was adjusted with hydrogen chloride and was equilibrated overnight inside an incubator set at 5% CO_2. To attain pH 6.5, 42 μL of 1N hydrogen chloride was added per 1-mL medium; to attain pH 7.4, 27 μL of 1 N hydrogen chloride was added per 1 mL medium. The final pH was confirmed inside the incubator using a pH electrode connecting the pH meter (744 pH Meter, Metrohm Schweiz AG, Zofingen, Switzerland) set outside the incubator. Following a 72-hour exposure, cells were washed with Krebs-Ringer solution, maintained in pH 7.4 and O_2 20%, and evaluated for calcium imaging.

3. Preparation of IVD Conditioned Media

In addition to direct exposure of DRG cells to hypoxia and low pH ('direct influence'), hypoxia and low pH may promote the IVD to release metabolites, cytokines, and other factors in the IVD CM which sensitize DRG neurons ('indirect effect'). To study this sole 'indirect effect' and exclude the interference from 'direct effect', one must ensure that all IVD CM are normoxic and at neutral pH. To achieve this goal, after stimulating the IVDs using hypoxia and/or low pH for 3 days (preconditioning), the IVD culture medium was changed to normoxia and neutral pH for IVD CM collection.

In details, IVDs were dissected from 7 bovine tails obtained from a local abattoir. Whole IVDs were excised with intact endplates and were cultured in different hypoxic and/or acidic conditions (pH 7.4, O_2 20%; pH 6.5, O_2 20%; pH 7.4, O_2 2%; and pH 6.5, O_2 2%) in DMEM with 0.11-g/L sodium pyruvate, 10% FCS and 1% P/S for 3 days. The pH adjustment methods were

https://doi.org/10.14245/ns.2040052.026

the same as described above. The donor and IVD size were evenly distributed between groups. After 3 days of culture, the culture medium of all discs was replaced by DMEM supplemented with 2% HEPES (Thermo Fisher Scientific; cat. no. 15630122) and cultured in 20% O_2 for additional 24 hours. Then these media (used for the last 24 hours of IVD culture in all groups) were collected and stored undiluted at -20°C until further use. These media contain metabolites, growth factors, and extracellular matrix proteins secreted into the media by the IVDs and were defined as the IVD conditioned media.

4. Indirect, IVD-Mediated Exposure of ND7/23 Cells to Different Combinations of pH and Oxygen Level

ND7/23 cells were seeded in 48-well plates at a density of 10,000 cells/cm^2. After 1 hour of cell attachment in standard culture conditions (pH 7.4, O_2 20%, cultured in DMEM with 0.11-g/L sodium pyruvate, 10% FCS and 1% P/S), the culture medium was replaced by the different undiluted IVD CM. In addition, 0.5% FCS, 1 mM cAMP and 10 ng/mL (NGF) were added to all the groups to induce neural differentiation. After 72 hours of culture, calcium imaging was performed. The DRG cell line treatment was limited to 72 hours because longer time in low serum conditions caused a significant cell death.

5. Calcium Imaging

The calcium imaging method was based on former literature.[36] The cells were washed with Krebs-Ringer's solution (NaCl 119 mM, KCl 2.5 mM, NaH_2PO_4 1.0 mM, $CaCl_2$ 2.5 mM, $MgCl_2$ 1.3 mM, HEPES 20 mM and D-glucose 11.0 mM dissolved in deionized water and filtered with 0.22-μm filter) and then incubated with 5 μM Fluo-4-AM (F14217; Thermo Fisher Scientific, Reinach, Switzerland) dissolved in Krebs-Ringer's solution supplemented with 0.3% bovine serum albumin (Fluka, Buchs, Switzerland; cat. no. 05484) and 10 μM probenecid (Thermo Fisher Scientific; cat. no. P36400) for 40 minutes at 37°C. Cells were washed once with Krebs-Ringer's solution and further incubated for 10 minutes at 37°C to de-esterize Fluo-4-AM. Following this step, cells were washed again and then preserved in 200-μL Krebs-Ringer solution. Time-lapse images were acquired using EVOS FL Auto 2 Imaging System (Thermo Fisher Scientific) at ×20 magnification, 0.40 numerical aperture and 6.8-mm working distance. The image acquisition rate was set at one image per second and the recording time was set to 200 seconds. The first 100 seconds were taken as baseline level. At the 100th second, 200 μL of 1 μM bradykinin (Sigma-Aldrich; cat. no. B3259) was added to the well (bradykinin final concentration = 0.5 μM) to study the DRG cell line response to bradykinin.

6. Calcium Imaging Data Analysis

Since in animal models nerve fibers (neurite outgrowth) were frequently evaluated for their extracellular discharge to study the physiological mechanism of pain,[14,15] in our vitro study calcium signal in the neurite outgrowth was assessed in addition to the evaluation of calcium signal in the soma (Fig. 1C-E). The calcium imaging method was modified based on previously reported protocols and includes 3 steps: (1) definition of the region of interest (ROI), (2) normalization of the fluorescent change over time, and (3) analysis of the calcium fluorescent peaks.[37,38]

ROI of soma was automatically established using a threshold of '20-255' in the 8-bit stack image produced by 'Z project' function within ImageJ Fiji (version 1.52p, National Institutes of Health, Bethesda, MD, US) using time-lapse images from 1 to 100 seconds with the projection type set as 'average intensity.' Since cell loading of Fluo-4-AM depends on intracellular esterase activity of living cells, this method can be used to exclude non-viable cells (fluorescent intensity below the threshold).

The longest neurite outgrowth per cell was defined as ROI of outgrowth using the 'Simple Neurite Tracer' plugin (ver. 3.1.3) within ImageJ Fiji[39] in the 8-bit stack image. The stacked image was acquired using the 'Z project' function from 1 to 200 seconds, with projection type set as 'maximum intensity.' This was done to achieve a high sensitivity for recognizing fine outgrowth. Only outgrowth longer than 30 μm (which is approximately the soma diameter) was included in the analysis. Since outgrowths collapse when cells die, the calcium imaging within outgrowth should indicate living cell functions.

The mean value of fluorescent intensity within the ROI was analyzed as 'grey value' of images using the ImageJ Fiji. The 'grey value' was averaged in images from 1 to 100 seconds to obtain the baseline fluorescence level (F_0). The real-time fluorescent value (F) was normalized by F_0 to obtain the relative fluorescent change over time $(F-F_0)/F_0$. The calculation was performed using 'R' (versions 3.5.2 and 3.6.2 Lucent Technologies Inc., Reston, VA, USA), which was also used to plot first derivative curves of $\Delta F/F_0$ over time (representing the speed of relative fluorescence change over time).

Spontaneous activation of the cell line was evaluated from 1 to 100 seconds, while response to bradykinin was evaluated from 100 to 200 seconds. To filter out noise, only a fast increase of $\Delta F/F_0$ was considered an intracellular calcium event (i.e., calcium peak). Hence, the first derivative ($d\Delta F/F_0$) of the $\Delta F/F_0$ curve was used to represent how fast intracellular calcium concentration

was changing over time. Only if $d\Delta F/F_0$ was higher than 0.05/sec (fluorescent intensity changing faster than 0.05 of baseline level per second), the peak was considered as a calcium event.

7. Statistics

For both spontaneous and bradykinin-induced calcium events in soma or outgrowth, proportions of cells with a calcium event (calcium peak with $d\Delta F/F_0$ larger than 0.05/sec) were statistically compared between groups using chi-square method in R.

For each soma or outgrowth, the intensity of calcium peaks was quantified using average maximum fluorescent elevation speed (MFES, based on the peak height in the derivative curve) and calcium peak height (based on the area under curve in the derivative curve) for both spontaneous and bradykinin-stimulated calcium events. Additionally, the peak frequency was analyzed for spontaneous calcium events, while duration of the calcium peaks of $d\Delta F/F_0$ was evaluated for bradykinin-stimulated calcium events. Since peaks were usually convolved after bradykinin stimulus, duration of the peaks was a better indicator than peak frequency for the analysis of bradykinin-stimulated calcium peaks. These indicators were compared between groups using Wilcoxon rank sum test in R.

The calcium imaging method was the same comparing ND7/23 cells stressed by hypoxia/low pH and those treated with different IVD CMs. For the ND7/23 stressed by hypoxia/low pH, 5 independent experiments were performed, with 3 wells per group in each experiment. One field of each well was taken for the calcium imaging analysis. The data shown were pooled from the 5 independent experiments. For the ND7/23 treated with different IVD CMs, IVDs from 7 bovine tails were included (biological replicates), with 2–4 IVDs dissected from each tail. The CM from the same bovine donor and same group was combined to stimulate 3 wells of ND7/23 cells (technical replicates). One field per well was used for the calcium imaging analysis.

8. Sheep DRG Dissociated Cell Culture

Primary DRG cell culture from a large animal (sheep) was used to validate the main findings obtained with the ND7/23 cell line. DRGs were dissected from sheep lumbar spines (L1–5) (obtained from sheep used in other unrelated preclinical studies approved by the cantonal ethics committee of Graubünden/Grisons). After carefully removing the DRG membrane and mincing the DRGs into small pieces with a scalpel, cells were isolated by sequential digestion of the minced DRG tissues with 2.5-mg/mL type I collagenase (Sigma-Aldrich; C9896) in PBS (37°C, on a shaker) for 1 hour and 0.25% trypsin/EDTA (Gibco; cat. no. 15400-054) solution (prewarmed to 37°C) for another 30 minutes. Trituration of the loosened DRGs was performed using a pipette tip (100–1,000 μL) until the digested tissue pieces could easily pass through the pipette tip. The cell suspension was then filtered through a 100-μm cell strainer (Falcon, Corning, NY, USA) to eliminate undigested tissue clusters and the enzymatic activity was stopped using an equal volume of DMEM/F12 medium supplemented with 10% FCS. Cells were centrifuged once (200 g for 10 minutes) and resuspended in DMEM/F12 medium with 10% FCS. Cells dissociated from 12 DRGs (obtained from sheep lumbar spine) were resuspended in 4 mL solution and distributed into 12 wells of 15 μ-Slide 8 well chambers (ibidi GmbH, Gräfelfing, Germany; cat. no. 80824) (200-μL cell solution per well) with an overall culture surface of 12 cm^2. In this way an initial confluency of around 70% could be constantly achieved. Cells were seeded using 200 μL of cell suspension per well. Following an overnight incubation, half of the medium in one chamber was replaced with DMEM 10% FCS preadjusted to pH 6.5 and kept in 2% oxygen culture for another 4 days (as acidic/hypoxic group), while half of the medium in the other chamber was changed to DMEM 10% FCS preadjusted to pH 7.4 and cultured in 20% oxygen for additional 4 days (as neutral pH/normoxic group). Half of the medium was changed to pH-adjusted medium because the primary DRG neurons dramatically lost viability if the whole culture medium was replaced with medium adjusted to pH-6.5. Two independent experiments were performed using DRGs from 2 sheep donors; each group in each independent experiment included 6 wells of culture for calcium imaging.

9. Calcium Imaging of Sheep Primary DRG Cell Culture

The calcium imaging method for primary sheep DRG cells was mostly the same as for the ND7/23 cells. The only difference was an additional step to recognize neurons from other kinds of cells in the mixed DRG culture: following 0–100 seconds of baseline recording and 100–200 seconds bradykinin response recording, 30 μL of 500 mM potassium chloride was added to the DRG cells in 270-μL Krebs-Ringer solution at the 200th second for another 50-second recording. Since only neuronal structures depolarize due to extracellular increase of potassium chloride, ROIs obtained for the primary DRG cells using the same method as in cell line calcium imaging analysis were subdivided to those with potassium induced calcium peak (DRG neuronal structures) and those without potassium induced peak (nonneuronal structures) after adding potassium chloride (a peak was defined as $d\Delta F/F_0$ higher than 0.05/sec,

https://doi.org/10.14245/ns.2040052.026

the same as in the cell line data analysis).[40,41] The neuronal subdivision procedures were performed using 'R'. The proportion of neuronal ROIs with calcium events, average MFES and peak height were evaluated for both spontaneous and bradykinin-stimulated calcium events. The peak frequency was analyzed for spontaneous calcium events and flux duration was evaluated for bradykinin-stimulated calcium events.

RESULTS

1. Direct Exposure to Hypoxia and Low pH Promoted Spontaneous Calcium Response in ND7/23 Outgrowth and Soma

Ischemia in DRG can develop as a result of the exposure to the degenerative IVD microenvironment.[14,15] Therefore, hypoxia and low pH as ischemia-related factors were evaluated regarding their influence on DRG neuronal sensitization. Hypoxia and/or low pH increased spontaneous calcium response both in neurite outgrowth and soma, as it can be qualitatively observed in the first derivative of the fluorescence curves over time (Fig. 2A-D, Fig. 3A-D). This was further validated by the following quantifications of the calcium peaks in the curves.

For spontaneous calcium response in the neurite outgrowth, low pH alone significantly increased MFES, peak frequency and peak height by 4.1%, 75%, and 29.2%, respectively, while hypoxia alone only increased MFES by 29.3% (Fig. 2F-H). The combination of hypoxia with low pH resulted in a significant increase of MFES, frequency and height (by 12.7%, 50%, and 31.7%, respectively) compared to normoxia and neutral pH (Fig. 2F-H). No significant difference in proportion of cells with calcium events was found among groups (Fig. 2E).

For spontaneous calcium response in the soma, changes in pH alone or oxygen tension alone had only minor effects on MFES, peak frequency and peak height (Fig. 3F-H), but the

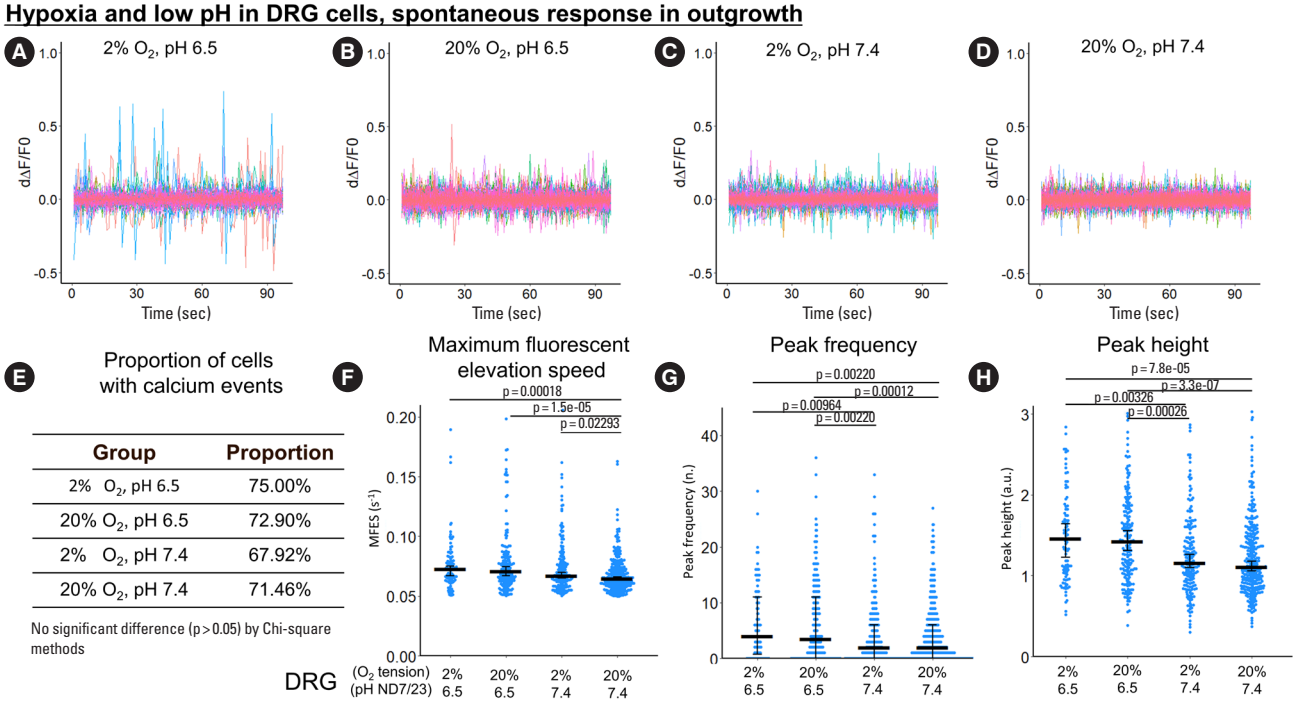

Fig. 2. The influence of hypoxia and low pH on spontaneous response (from 0 to 100 seconds) in ND7/23 outgrowth. (A-D) First derivative of the normalized fluorescence (ratio of F-F_0 and F_0), which indicates intracellular calcium concentration fluctuation. Each colored curve represents one neurite outgrowth from each cell. Peaks in the curve are regarded as calcium events which indicate neuronal discharge. Around 120 to 450 cells per group were included for this study. (E) Proportion of cells with calcium events. The definition of calcium event is the peak in the derivative curve larger than 0.05/sec. Chi-square method was used for statistics. (F-H) Maximum fluorescent elevation speed, peak frequency, and peak height were calculated based on the derivative curve. Blue spots in the plots show data distribution; black bar represents median; error bars in panels F and H show 95% confident interval of median (calculated using bootstrapping method); while error bar in panel G shows 25% and 75% quantile. A p-value was calculated using pairwise comparisons of Wilcoxon rank sum test. A value of $p < 0.05$ was regarded as significant and those values were shown in the plots. DRG, dorsal root ganglion.

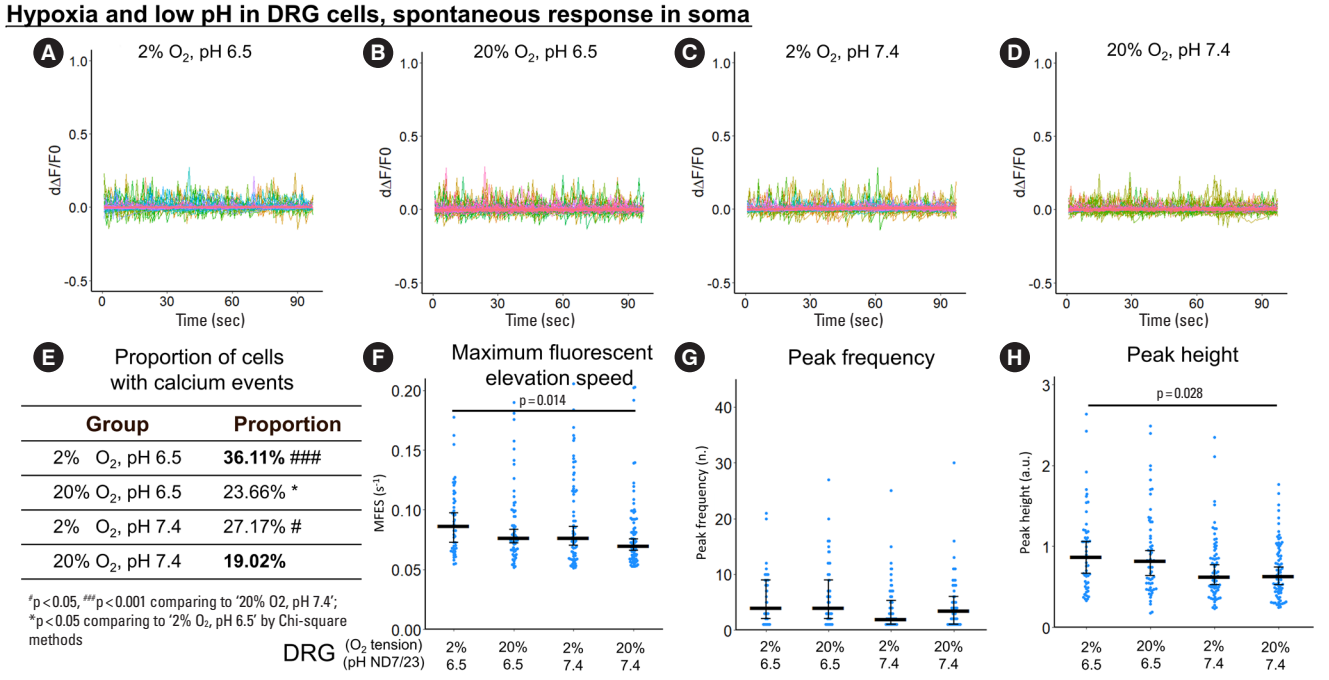

Fig. 3. The influence of hypoxia and low pH on spontaneous response (from 0 to 100 seconds) in ND7/23 soma. (A-D) First derivative of the normalized fluorescence (ratio of F-F_0 and F_0), which indicates intracellular calcium concentration fluctuation. Each colored curve represents one soma from each cell. Peaks in the curve are regarded as calcium events which indicate neuronal discharge. Around 120 to 450 cells per group were included for this study. (E) Proportion of cells with calcium events. The definition of calcium event is the peak in the derivative curve larger than 0.05/sec. Chi-square method was used for statistics. (F-H) Maximum fluorescent elevation speed, peak frequency, and peak height were calculated based on the derivative curve. Blue spots in the plots show data distribution; black bar represents median; error bars in panels F and H show 95% confident interval of median (calculated using bootstrapping method); while error bar in panel G shows 25% and 75% quantile. A p-value was calculated using pairwise comparisons of Wilcoxon rank sum test. A value of $p < 0.05$ was regarded as significant and those values were shown in the plots. DRG, dorsal root ganglion.

combination of hypoxia with low pH enhanced MFES and calcium peak height by 23.5% and 37.3% compared to normoxia and neutral pH (Fig. 3F, H), respectively. Hypoxia alone was enough to increase the proportion of cells with calcium events by 42.8% (from 19.02% to 27.17%) compared to normoxia and neutral pH ($p = 0.017$) (Fig. 3E), while the combination of hypoxia with low pH induced a significant increase in the proportion of reactive cells by 89.9% (from 19.02% to 36.11%) ($p < 0.001$) (Fig. 3E). Only minor changes in peak frequency were detected among groups (Fig. 3G).

2. Direct Exposure to Hypoxia and Low pH Promoted Bradykinin-Stimulated Response in ND7/23 Soma and Outgrowth

Overall, the bradykinin-stimulated response was stronger than spontaneous response (Fig. 4A-D, Fig. 5A-D), thus peak duration was evaluated instead of peak frequency (small peaks tend to convolve with each other). The calcium response to bradykinin stimulation was different in the outgrowth and soma regions.

Regarding the calcium response to bradykinin in neurite outgrowth, hypoxia, low pH and their combination all significantly increased MFES (by 46%, 37%, and 55.4%, respectively, Fig. 4F) compared to normoxia and neutral pH. Low pH alone increased calcium peak height by 19.8% (Fig. 4F), while low pH combined with hypoxia increased peak height by 39.7% (Fig. 4H) compared to normoxia and neutral pH. The proportion of reactive cells was higher than 90% in all bradykinin-stimulated groups (Fig. 4E). No significant difference was detected for peak duration among groups (Fig. 4G).

For bradykinin-stimulated response in soma, when ND7/23 was stressed by hypoxia and/or low pH, calcium flux was faster (indicated by the larger MFES) (Fig. 5F) but shorter (indicated by the smaller peak duration) (Fig. 5G), thus the peak height showed no significant difference among groups (Fig. 5H). The proportion of reactive cells was high in all bradykinin-stimulated groups (Fig. 5E). Representative images of calcium imaging

https://doi.org/10.14245/ns.2040052.026

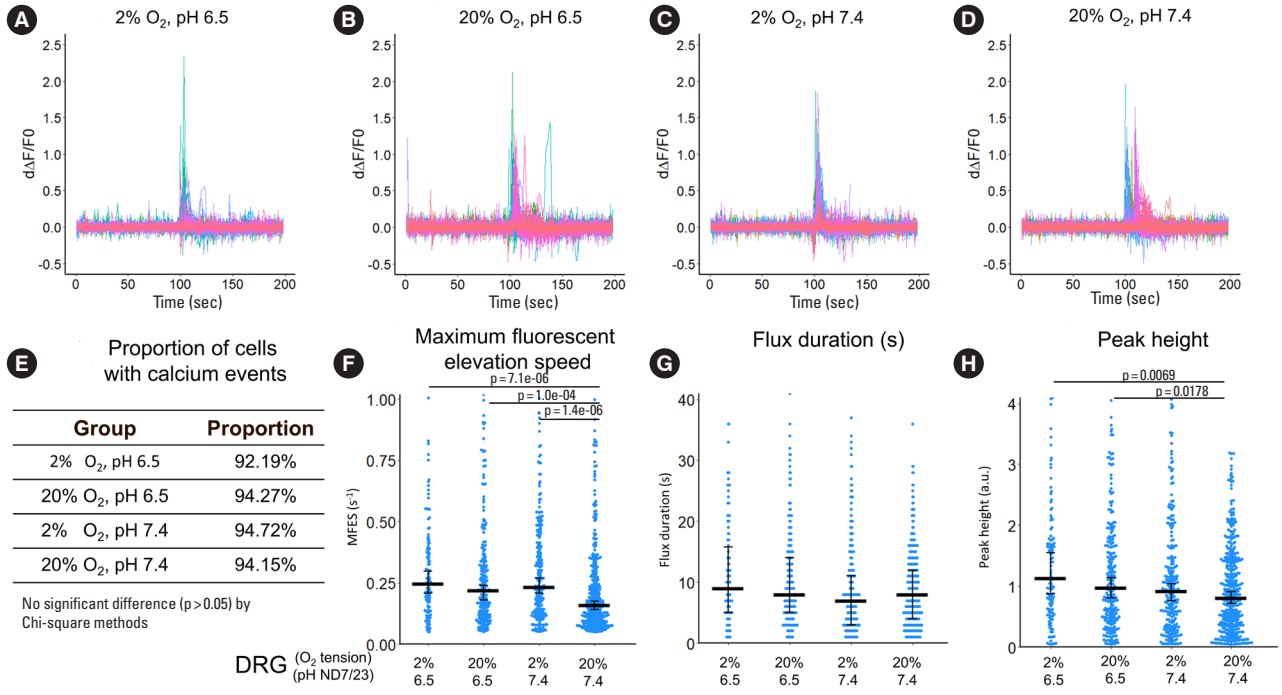

Fig. 4. The influence of hypoxia and low pH on bradykinin-stimulated response (from 0 to 100 seconds) in ND7/23 outgrowth. (A-D) First derivative of the normalized fluorescence (ratio of F-F_0 and F_0), which indicates intracellular calcium concentration fluctuation. Each colored curve represents one neurite outgrowth from each cell. Peaks in the curve are regarded as calcium events which indicate neuronal discharge. Around 120 to 450 cells per group were included for this study. (E) Proportion of cells with calcium events. The definition of calcium event is the peak in the derivative curve larger than 0.05/sec. Chi-square method was used for statistics. (F-H) Maximum fluorescent elevation speed, peak frequency, and peak height were calculated based on the derivative curve. Blue spots in the plots show data distribution; black bar represents median; error bars in panels F and H show 95% confident interval of median (calculated using bootstrapping method); while error bar in panel G shows 25% and 75% quantile. A p-value was calculated using pairwise comparisons of Wilcoxon rank sum test. A value of $p < 0.05$ was regarded as significant and those values were shown in the plots. DRG, dorsal root ganglion.

at the time of bradykinin addition are shown in Fig. 5I-L and representative videos are provided as Supplementary vedio clips 1 and 2.

3. Indirect, IVD-Mediated Exposure to Hypoxia and Low pH Promoted Spontaneous Calcium Response in ND7/23 Outgrowth

Since DRG neurites extend to the outer portion of the IVD, hypoxia and low pH in the IVD can indirectly influence the DRG, representing a possible mechanism of DRG sensory neuron sensitization. To study this effect, ND7/23 cells were treated with hypoxia-acidosis-stressed IVD CM or nonstressed IVD CM, and calcium response was investigated through the calcium peaks (calcium events) shown in the derivative curve of normalized fluorescence over time (Fig. 6A-D, Fig. 7A-D).

Overall, the indirect, IVD-mediated effect of the combination of acidosis and hypoxia on DRG sensitization was similar to the direct effect. Generally, MFES, peak frequency and peak height were the highest in this group for both spontaneous and bradykinin-stimulated calcium response in the outgrowth.

Specifically, in the neurite outgrowth, hypoxia-acidosis-stressed IVD CM significantly increased the spontaneous calcium response of ND7/23 cells compared to nonstressed IVD CM. Calcium peak frequency and peak height were all significantly elevated by hypoxia-acidosis-stressed IVD CM (increased by 37.5% and 23.4%, respectively) (Fig. 6G, H), which was intuitively shown in the derivative curve of normalized fluorescence over time (Fig. 6A-D). No significant difference was found between groups regarding proportion of cells with response and MFES (Fig. 6E, F).

In the soma, spontaneous calcium response was also the highest in the hypoxia-acidosis-stressed IVD CM group, although

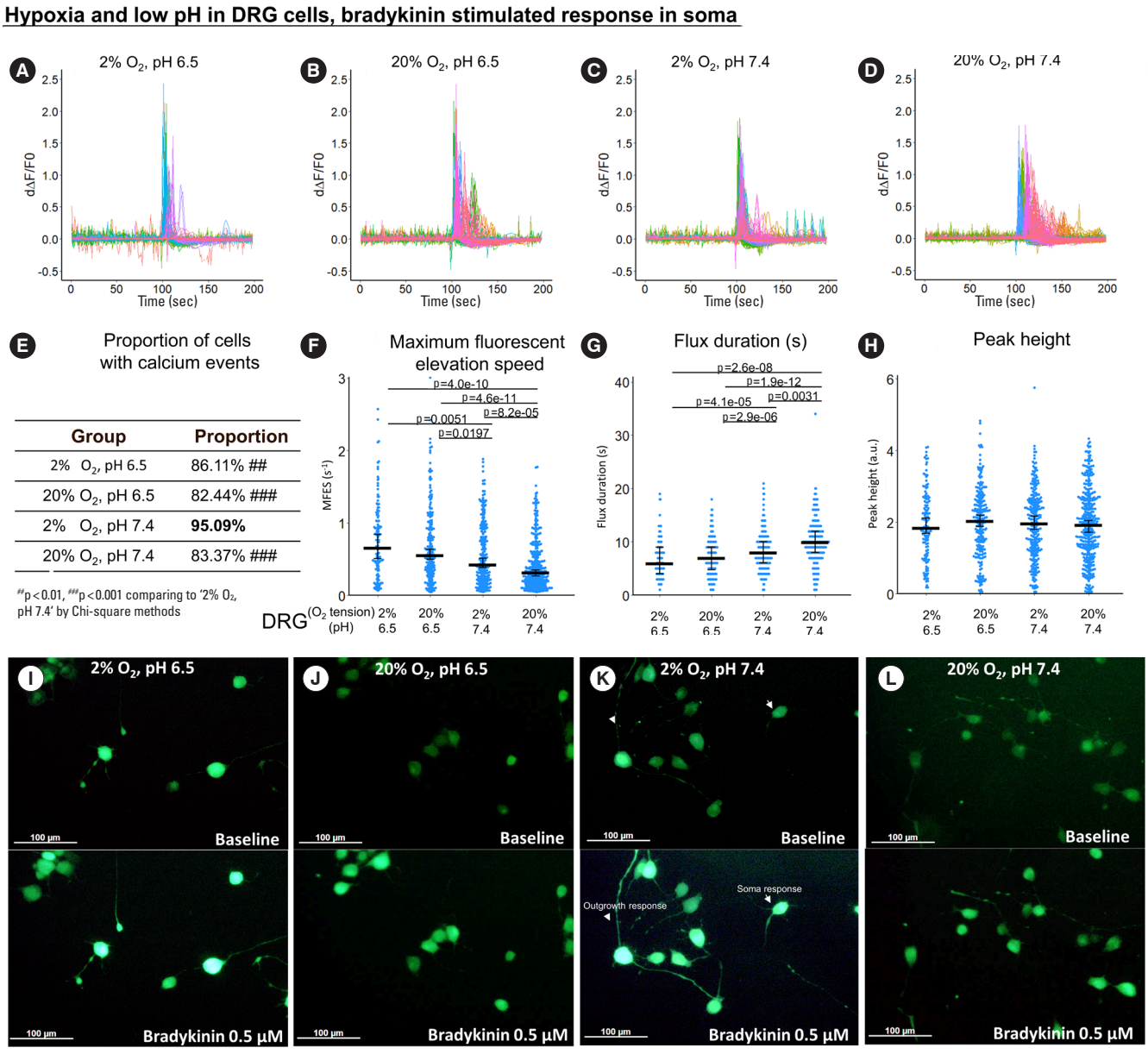

Fig. 5. The influence of hypoxia and low pH on bradykinin-stimulated response (from 0 second to 100 seconds) in ND7/23 soma. (A-D) First derivative of the normalized fluorescence (ratio of F-F_0 and F_0), which indicates intracellular calcium concentration fluctuation. Each colored curve represents one soma from each cell. Peaks in the curve are regarded as calcium events which indicate neuronal discharge. Around 120 to 450 cells per group were included for this study. (E) Proportion of cells with calcium events. The definition of calcium event is the peak in the derivative curve larger than 0.05/sec. Chi-square method was used for statistics. (F-H) Maximum fluorescent elevation speed, peak frequency, and peak height were calculated based on the derivative curve. Blue spots in the plots show data distribution; black bar represents median; error bars in panels F and H show 95% confident interval of median (calculated using bootstrapping method); while error bar in panel G shows 25% and 75% quantile. A p-value was calculated using pairwise comparisons of Wilcoxon rank sum test. A value of $p < 0.05$ was regarded as significant and those values were shown in the plots. (I-L) Examples of images before (baseline) and at 0.5 μM bradykinin stimulation in the calcium imaging time-lapse sequence. Arrows in panel K indicate soma calcium response, while arrow heads in panel K indicate outgrowth calcium signal responding to bradykinin. Scale bars equal to 100 μm. DRG, dorsal root ganglion.

https://doi.org/10.14245/ns.2040052.026

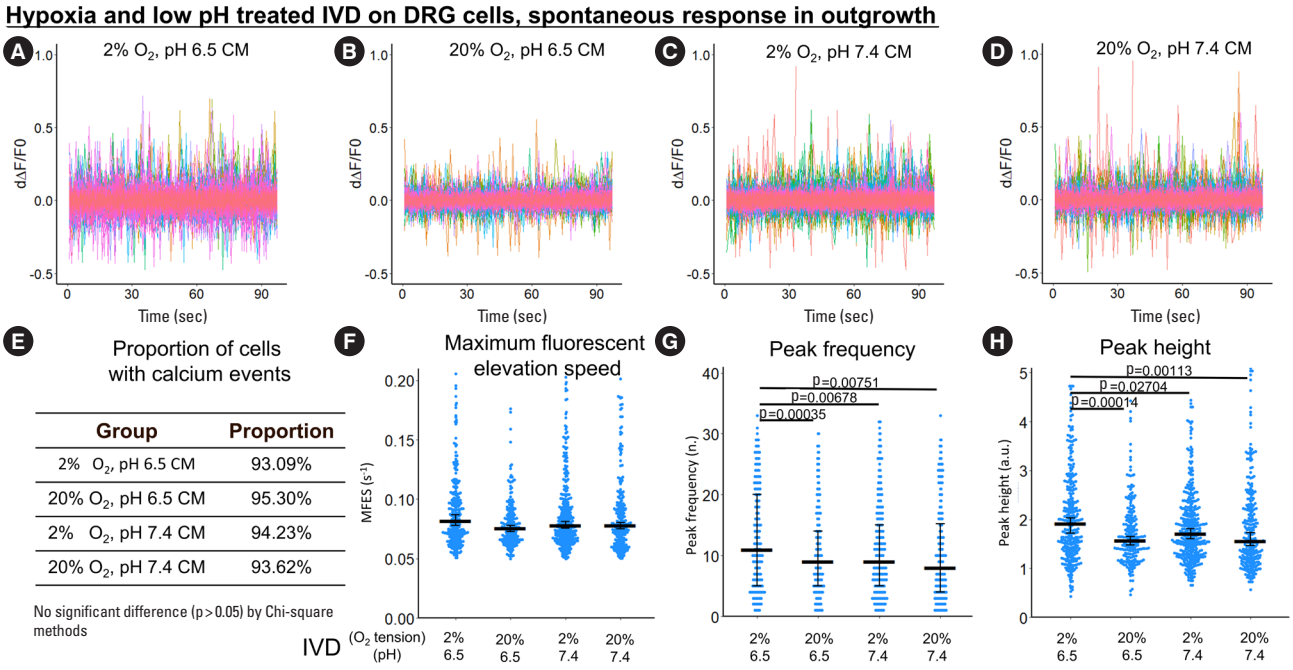

Fig. 6. The influence of hypoxia-acidosis-stressed IVD CM on spontaneous response (from 0 to 100 seconds) in ND7/23 outgrowth. (A-D) First derivative of the normalized fluorescence (ratio of F-F_0 and F_0), which indicates intracellular calcium concentration fluctuation. Each colored curve represents one neurite outgrowth from each cell. Peaks in the curve are regarded as calcium events which indicate neuronal discharge. Around 120 to 450 cells per group were included for this study. (E) Proportion of cells with calcium events. The definition of calcium event is the peak in the derivative curve larger than 0.05/sec. Chi-square method was used for statistics. (F-H) Maximum fluorescent elevation speed, peak frequency, and peak height were calculated based on the derivative curve. Blue spots in the plots show data distribution; black bar represents median; error bars in panels F and H show 95% confident interval of median (calculated using bootstrapping method); while error bar in panel G shows 25% and 75% quantile. A p-value was calculated using pairwise comparisons of Wilcoxon rank sum test. A value of $p < 0.05$ was regarded as significant and those values were shown in the plots. IVD, indirectly via intervertebral disc; CM, conditioned medium; DRG, dorsal root ganglion.

the differences were smaller than in the outgrowth region (Fig. 7).

4. Indirect, IVD-Mediated Exposure to Hypoxia and Low pH Enhanced Bradykinin-Stimulated Calcium Response in ND7/23 Outgrowth

To study the sensitivity of the DRG cell line in response to an inflammatory cytokine, bradykinin-triggered calcium response in both soma and outgrowth was evaluated after treatment with IVD CM. Overall, the trends were similar to the ones observed for the DRG cultures directly exposed to hypoxia and/or acidosis.

Specifically, in the outgrowth, the proportion of cells with calcium events, MFES, flux duration and peak height were increased by 7.8%, 17.4%, 33.3%, and 36.3%, respectively by hypoxia-acidosis-stressed IVD CM compared to nonstressed IVD CM (Fig. 8E-H).

Changes in oxygen tension seemed to have a stronger indirect effect on the calcium response of ND7/23 cells in the outgrowth compared to changes in pH: CM of IVD stressed by hypoxia alone was enough to enhance proportion of cells with calcium events, MFES, flux duration and peak height by 5.6%, 19.3%, 22.2%, and 23.6%, respectively comparing to nonstressed IVD CM (Fig. 8E-H). CM of IVD stressed by acidosis alone increased the proportion of cells with calcium events by 8.1% (Fig. 8E) but had only minor effects on other indicators.

In the soma, calcium response to bradykinin showed no significant difference among groups (Fig. 9).

5. Hypoxia and Low pH Promoted Both Spontaneous and Bradykinin-Stimulated Response in Sheep DRG Neurons

Based on the results obtained with the neural cell line, direct exposure of DRGs to hypoxia and low pH showed a stronger effect on DRG neuronal sensitization compared to indirect, IVD-mediated exposure to the same stimuli. Hence, in the primary sheep DRG neuronal cultures, only the direct effects of

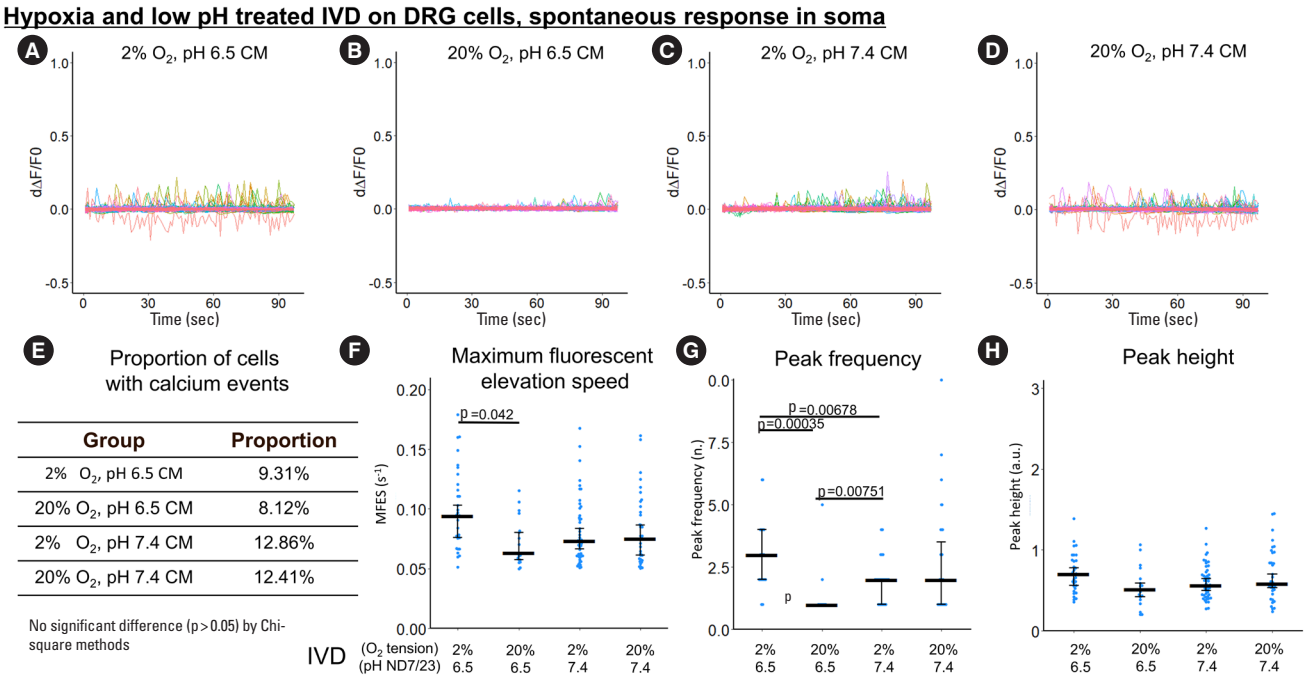

Fig. 7. The influence of hypoxia-acidosis-stressed IVD CM on spontaneous response (from 0 to 100 seconds) in ND7/23 soma. (A-D) First derivative of the normalized fluorescence (ratio of F-F_0 and F_0), which indicates intracellular calcium concentration fluctuation. Each colored curve represents one soma from each cell. Peaks in the curve are regarded as calcium events which indicate neuronal discharge. Around 120 to 450 cells per group were included for this study. (E) Proportion of cells with calcium events. The definition of calcium event is the peak in the derivative curve larger than 0.05/sec. Chi-square method was used for statistical analysis. (F-H) Maximum fluorescent elevation speed, peak frequency, and peak height were calculated based on the derivative curve. Blue spots in the plots show data distribution; black bar represents median; error bars in panels F and H show 95% confident interval of median (calculated using bootstrapping method); while error bar in panel G shows 25% and 75% quantile. A p-value was calculated using pairwise comparisons of Wilcoxon rank sum test. A value of $p<0.05$ was regarded as significant and the values are shown in the plots. IVD, indirectly via intervertebral disc; CM, conditioned medium; DRG, dorsal root ganglion.

hypoxia and low pH were investigated. Overall, the combined effect of acidosis and hypoxia was similar in primary DRG neurons and ND7/23 cells.

Specifically, spontaneous peak height of neuronal structures in hypoxia and low pH culture was 24.7% higher than those in normoxia and neutral pH culture (Fig. 10F). For bradykinin-stimulated response in neuronal structures, proportion of cells with calcium events in hypoxia and low pH culture was 11.2% higher than those in normoxia and neutral pH culture (Fig. 10I). Hypoxia and low pH induced higher MFES but lower flux duration, thus peak height showed no significant difference (Fig. 10J-L).

For spontaneous calcium response in nonneuronal structures, hypoxia and low pH treatment did not seem to have a strong influence: the proportion of cells with calcium events was only increased by 6.3% (Fig. 11C), while MFES and peak height was decreased by 3.7% and 0.8%, respectively (Fig. 11D, F). For bradykinin-stimulated calcium response, hypoxia and low pH decreased MFES, flux duration and peak height by 72.2%, 66.7%, and 69.8%, respectively (Fig. 11J-L).

DISCUSSION

In this study, insufficient blood supply was hypothesized to be a causative factor in discogenic pain. Atherosclerotic lesions in the abdominal aorta and cardiovascular risk factors were constantly found to be correlated with LBP.[4,6,42] However, to the best of our knowledge, the ischemia-related discogenic pain has not been successfully modelled in preclinical research, making it challenging to study the underlying biological and physiological mechanisms and screen for novel treatments.

In the current *in vitro* system, DRG neurons could be sensitized by the microenvironment of IVD stressed by hypoxia and acidosis, which represents a mechanism of neuronal sensitization via IVD ischemia. On the other hand, ischemia in DRG

 https://doi.org/10.14245/ns.2040052.026

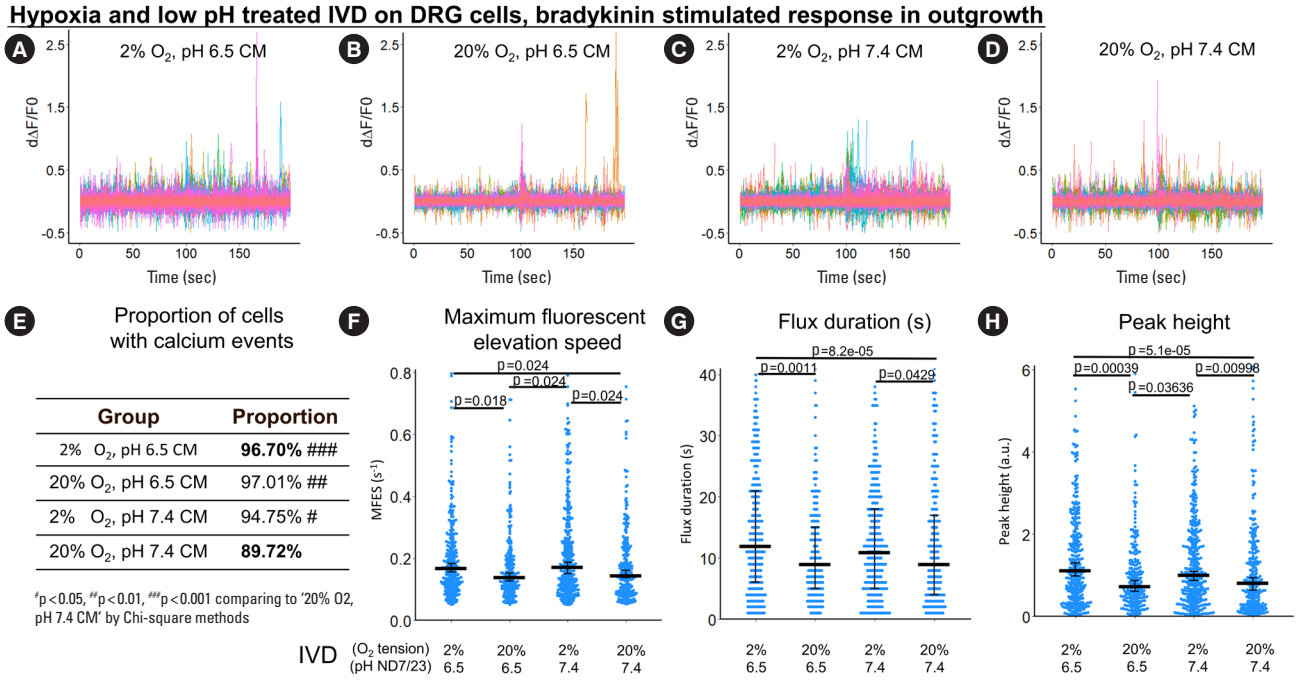

Group	Proportion
2% O_2, pH 6.5 CM	**96.70% ###**
20% O_2, pH 6.5 CM	97.01% ##
2% O_2, pH 7.4 CM	94.75% #
20% O_2, pH 7.4 CM	**89.72%**

#p<0.05, ##p<0.01, ###p<0.001 comparing to '20% O2, pH 7.4 CM' by Chi-square methods

Fig. 8. The influence of hypoxia-acidosis-stressed IVD CM on bradykinin-stimulated response (from 0 second to 100 seconds) in ND7/23 outgrowth. (A-D) First derivative of the normalized fluorescence (ratio of F-F_0 and F_0), which indicates intracellular calcium concentration fluctuation. Each colored curve represents one neurite outgrowth from each cell. Peaks in the curve are regarded as calcium events which indicate neuronal discharge. Around 120 to 450 cells per group were included for this study. (E) Proportion of cells with calcium events. The definition of calcium event is the peak in the derivative curve larger than 0.05/sec. Chi-square method was used for statistics. F-H Maximum fluorescent elevation speed, peak frequency, and peak height were calculated based on the derivative curve. Blue spots in the plots show data distribution; black bar represents median; error bars in panels F and H show 95% confident interval of median (calculated using bootstrapping method); while error bar in panel G shows 25% and 75% quantile. A p-value was calculated using pairwise comparisons of Wilcoxon rank sum test. A value of $p < 0.05$ was regarded as significant and those values were shown in the plots. IVD, indirectly via intervertebral disc; CM, conditioned medium; DRG, dorsal root ganglion.

was modelled by directly applying hypoxia and/or acidosis to the DRG neurons and seemed to have a stronger effect in promoting neuronal sensitization. These results indicate that besides the molecules produced by the IVD, ischemia-related hypoxia and acidosis in DRG themselves play a key role in neuronal sensitization.

According to the International Association for the Study of Pain (IASP), neuronal sensitization is defined as "an increased responsiveness of nociceptive neurons to their normal input, and/or recruitment of a response to normally subthreshold inputs, including spontaneous discharges".[43] In our study, neuronal sensitization was evaluated using spontaneous and bradykinin-stimulated calcium response. A transient increase of cytoplasmic calcium concentration reflects neuronal discharge, is necessary for neural transmitter release, and represents nociceptive/painful input to the CNS.[16,31] While spontaneous neuronal discharge is an important mechanism in spontaneous pain (defined as resting or ongoing pain),[17,44] the neuronal response to bradykinin indicates its nociceptive responsiveness in the context of inflammation[45] (the latter contributing to IVD degeneration and pain development).[46] Tissue damage and inflammation are accompanied by bradykinin release which was not only shown to be responsible for acute and chronic pain, but can also directly activate nociceptors.[45] Thus, evaluating responsiveness to bradykinin represents an important aspect in the evaluation of peripheral sensitization.[47]

The proportion of cells having spontaneous calcium response indicates the likelihood of "spontaneous discharges," while peak frequency and height show their intensity. A higher proportion of cells responding to bradykinin represents a lower threshold of calcium response under the same amount of bradykinin stimulus, while height of the calcium peak indicates the intensity of the bradykinin-stimulated response and is determined by both flux speed and flux duration. A higher calcium response

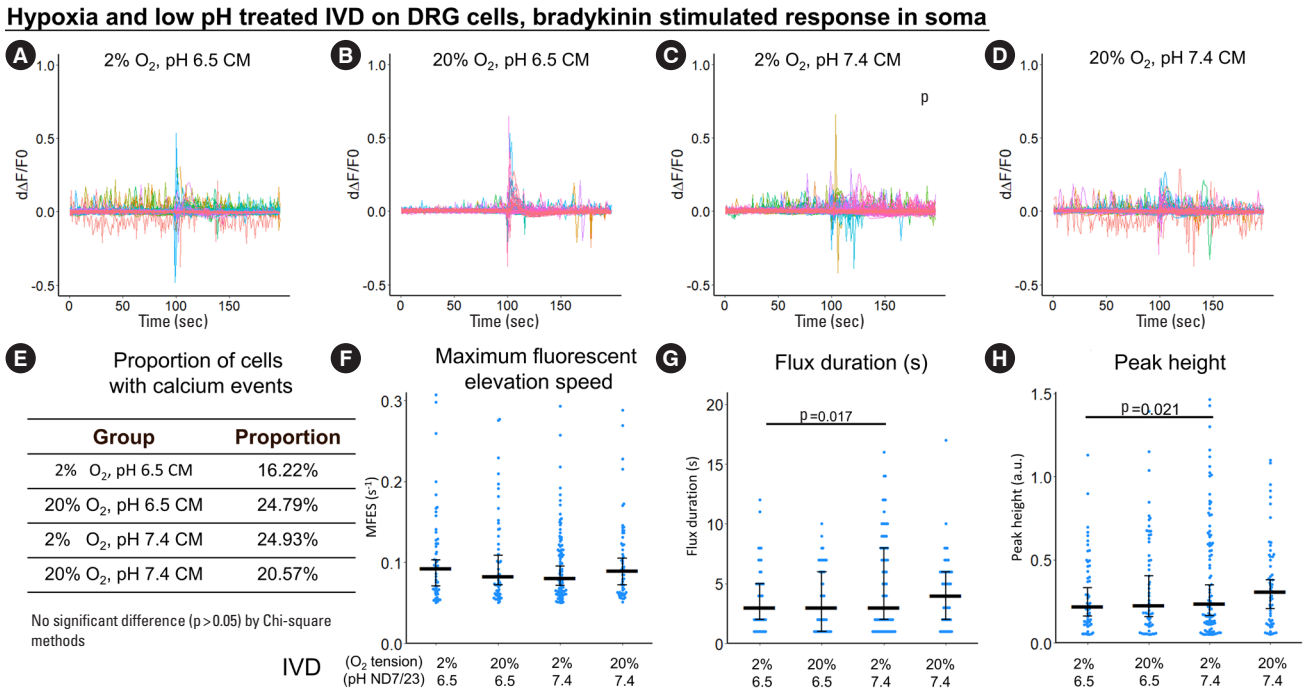

Fig. 9. The influence of hypoxia-acidosis-stressed IVD CM on bradykinin-stimulated response (from 0 second to 100 seconds) in ND7/23 soma. (A-D) First derivative of the normalized fluorescence (ratio of F-F_0 and F_0), which indicates intracellular calcium concentration fluctuation. Each colored curve represents one soma from each cell. Peaks in the curve are regarded as calcium events which indicate neuronal discharge. Around 120 to 450 cells per group were included for this study. (E) Proportion of cells with calcium events. The definition of calcium event is the peak in the derivative curve larger than 0.05/sec. Chi-square method was used for statistics. (F-H) Maximum fluorescent elevation speed, peak frequency, and peak height were calculated based on the derivative curve. Blue spots in the plots show data distribution; black bar represents median; error bars in panels F and H show 95% confident interval of median (calculated using bootstrapping method); while error bar in panel G shows 25% and 75% quantile. A p-value was calculated using pairwise comparisons of Wilcoxon rank sum test. A value of $p < 0.05$ was regarded as significant and those values were shown in the plots. IVD, indirectly via intervertebral disc; CM, conditioned medium; DRG, dorsal root ganglion.

detected using calcium imaging in large population of cells may indicate neuronal sensitization under direct or indirect stimulus of hypoxia and acidosis. However, care should be taken in the interpretation of calcium imaging results since: (1) Absolute speed of the short and transient calcium flux cannot be measured precisely since it takes relatively more time for the calcium and indicator reactions to reach equilibrium.[48,49] Nonetheless, the fluorescent elevation speed calculated from calcium imaging is still of value. Since a higher calcium flux speed is associated with a higher fluorescent elevation speed in calcium imaging,[49] the relative difference of fluorescent elevation speed among groups could reflect a difference in calcium flux. The absolute calcium flux speed cannot be measured exactly using calcium imaging, but it is possible to use calcium imaging for relative comparison. (2) Regarding neuronal discharge, it can only be approximated by calcium transient, and calcium imaging is only an indirect method for the measurement with a slower dynamic compared to patch clamp evaluation.[33] Other techniques such as patch clamp are therefore needed for more in-depth analyses in the future.

Acute pain is generally benign and self-limiting. The difficulties in pain management and treatment arise when pain becomes recurrent and/or chronic. Chronic pain has been recognized as that pain which persists past the normal time of healing.[50] For LBP, lack of recovery within 6 weeks, irrespective of the treatment type, is generally considered as chronic.[51] To understand how pain is sustained, we used a study design in which 'preconditioning' by hypoxia and low pH stress on the IVD was replaced by normoxia and neutral pH when preparing the IVD CM to mimic the "recovery" in the definition of chronic pain. We found that the IVD kept on forming the microenvironment promoting neural sensitization even after isch-

https://doi.org/10.14245/ns.2040052.026

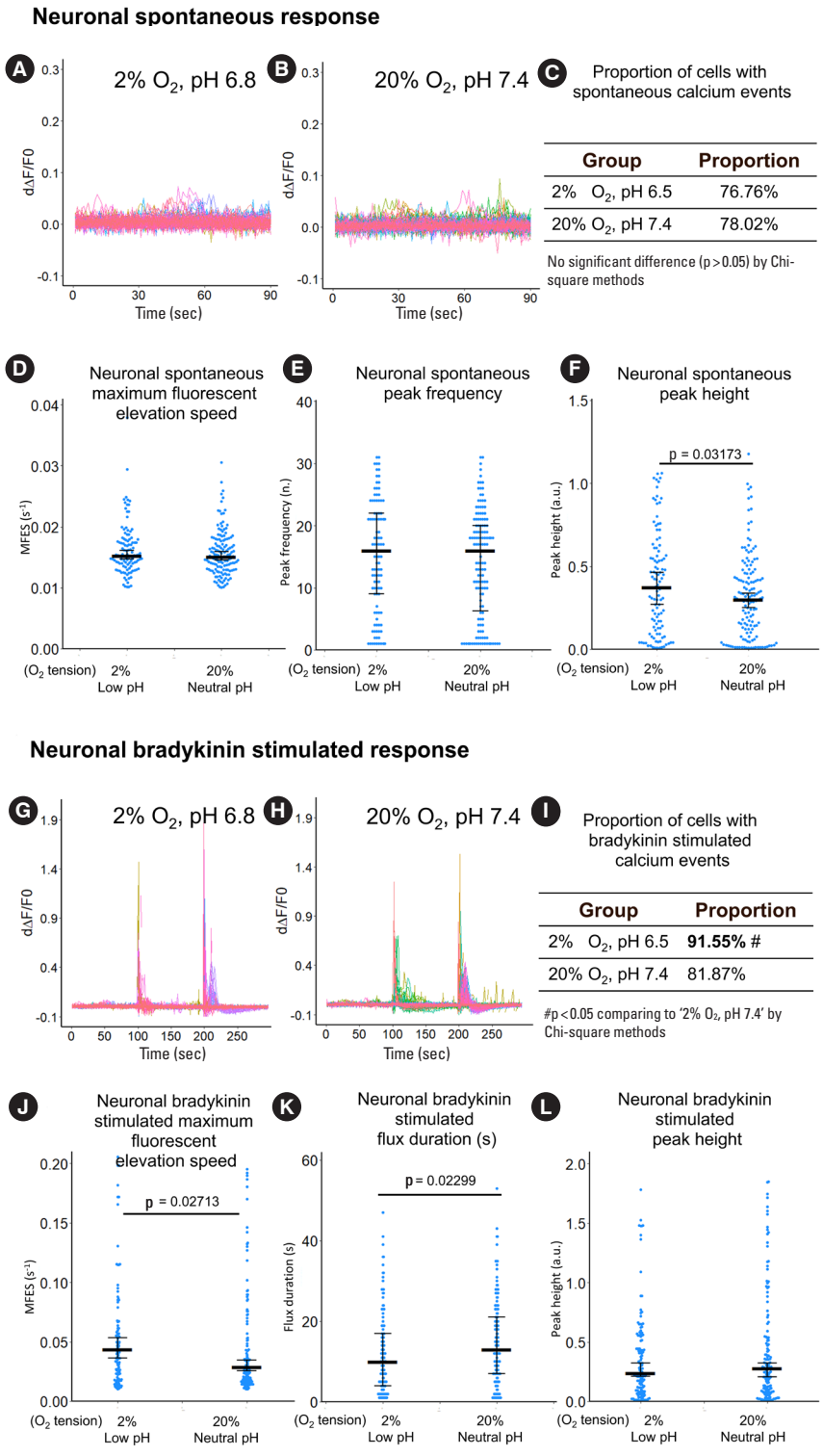

Fig. 10. The influence of hypoxia and low pH on calcium response of primary sheep DRG neuron. (A, B) Derivative fluorescent curve from 0 to 90 seconds which represent spontaneous response of the neurons. Each colored curve represents one neuronal structure. (C-F) Quantification of the spontaneous response using proportion of cells with calcium events, maximum fluorescent elevation speed, peak frequency, and peak height based on the derivative curve. (G, H) Derivative of fluorescent curve from 0 to 300 seconds. Bradykinin (0.5 μM) was added at the 100 seconds to evaluate the bradykinin-stimulated response while potassium chloride (50 mM) was added at the 200 seconds to differentiate neuronal structures from nonneuronal structures. Each curve represents one neuronal structure. (I-L) Quantification of the bradykinin-stimulated response using proportion of cells with calcium events, maximum fluorescent elevation speed, flux duration, and peak height based on the derivative curve. For panels A, B, G, H, peaks in the curve are regarded as calcium events which indicate neuronal discharge. The y-axis is the derivative level of normalized fluorescent (ratio of F-F_0 and F_0). Around n = 140 to 180 neuronal structures per group were included for this study. For panels C, I, the definition of calcium event is the peak in the derivative curve larger than 0.05/sec. Chi-square method was used for statistics. For panels D, E, F, J, K, L, blue spots in the plots show data distribution; black bar represents median; error bars in panels D, F, J, and L show 95% confident interval of median (calculated using bootstrapping method); while error bar in panels E and K show 25% and 75% quantile. A p-value was calculated using pairwise comparisons of Wilcoxon rank sum test. A value of $p < 0.05$ was regarded as significant and those values were shown in the plots. IVD, indirectly via intervertebral disc; CM, conditioned medium; DRG, dorsal root ganglion.

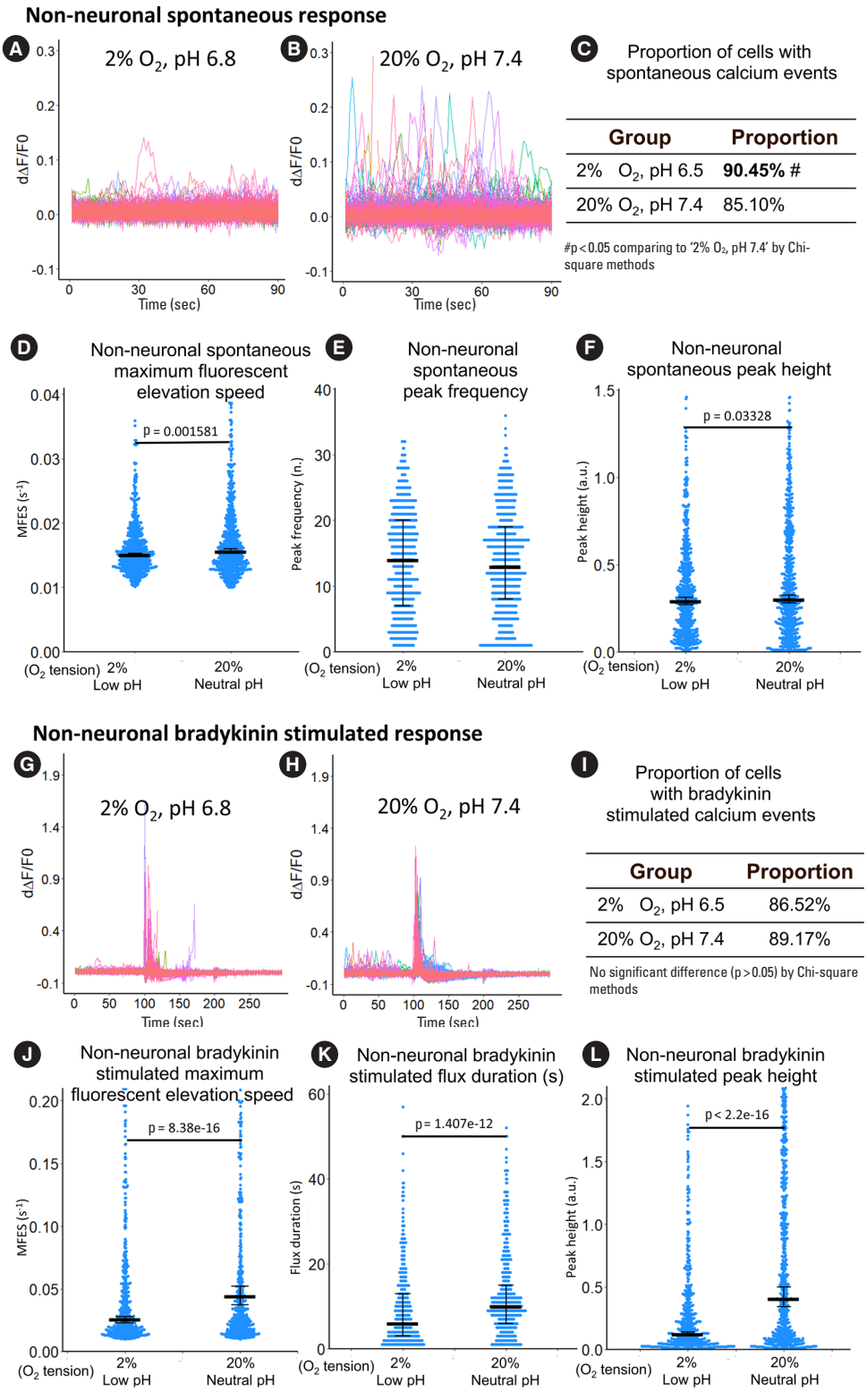

Fig. 11. The influence of hypoxia and low pH on calcium response of primary sheep DRG nonneuronal structures. (A, B) Derivative of fluorescent curve from 0 to 90 seconds which represent spontaneous response of the nonneuronal structures. Each colored curve represents one nonneuronal structure. (C-F) Quantification of the spontaneous response using proportion of cells with calcium events, maximum fluorescent elevation speed, peak frequency, and peak height based on the derivative curve. (G, H) Derivative of fluorescent curve from 0 to 300 seconds. Bradykinin (0.5 μM) was added at the 100 seconds to evaluate the bradykinin-stimulated response while potassium chloride (50 mM) was added at the 200 seconds (Nonneurons do not have instant response to extracellular rise of potassium.). Each curve represents one nonneuronal structure. (I-L) Quantification of the bradykinin-stimulated response using proportion of cells with calcium events, maximum fluorescent elevation speed, peak frequency, and peak height based on the derivative curve. For panels A, B, G, H, peaks in the curve are regarded as calcium events which indicate event of intracellular calcium rise. The *y*-axis is the derivative level of normalized fluorescent (ratio of F-F_0 and F_0). Around n = 660 to 785 nonneuronal structures per group were included for this study. For panels C, I, the definition of calcium event is the peak in the derivative curve larger than 0.05/sec. Chi-square method was used for statistics. For panels D, E, F, J, K, L, blue spots in the plots show data distribution; black bar represents median; error bars in panels D, F, J, and L show 95% confident interval of median (calculated using bootstrapping method); while error bars in panels E and K show 25% and 75% quantile. A value of $p < 0.05$ was regarded as significant and those values were shown in the plots. DRG, dorsal root ganglion.

https://doi.org/10.14245/ns.2040052.026

emia-related factors were removed. This study differs from other studies where sensitization was recorded under the stimulus and can be interpreted as a passive response to the stimulus.[52] Retrieving stress or other treatments during the recording suggests a prolonged effect which is not simply a passive response to noxious stimulus but may persist even after the stimulus is removed.

This study has several limitations: (1) it does not reflect the duration of the neural sensitization; (2) other mechanisms of pain persistence such as central sensitization and glial modulation etc.[53,54] were not addressed; (3) our *in vitro* model lacks the ability to reproduce the modulation from the CNS at tissue or organ level. Hence, the knowledge obtained *in vitro* requires further validation in preclinical and clinical studies.

Nerve fiber was frequently evaluated for its extracellular discharge in animal models to study physiological mechanisms of pain.[14,15] Therefore, the calcium response in both soma and neurite outgrowth was evaluated in our DRG cell line culture. Our results suggest that the outgrowth is more sensitive to changes in calcium signal than the soma. Hence, small changes caused either by a change in a single parameter in direct exposure (hypoxia alone or low pH alone) or by indirect effect (mediated by IVD CM) may be only detectable in the outgrowth. If the calcium imaging analysis had only been performed in soma, smaller influence caused by the treatment may have been overlooked, which further emphasized the necessity of recording neuronal discharge in neurite outgrowth specifically. As reported by Ladewig et al.,[55] outgrowth calcium transients may differ from somatic responses in their kinetics, amplitude, voltage dependence and regulation of basal calcium levels. This difference may be due to a higher enrichment of calcium channels at the nerve terminals compared to the soma.[56]

While the translational value of a cell line study is lower than in vivo studies, it does not require experimental animals. In this study, the cell line was used for preliminary screening and only validation of most representative findings was done in primary cultures from animals (sheep) already enrolled in unrelated preclinical studies. In this way, the number of experimental animals was reduced, preventing animal suffering and distress in the studies on pain, in line with 3R principles.

CONCLUSIONS

Hypoxia and low pH in the IVD or DRG may contribute to the development of peripheral neural sensitization, an important mechanism of pain. These results suggest alleviation of ischemia from DRG and IVD as a strategy against peripheral nerve sensitization. In addition to considering approaches against the degenerative IVD microenvironment, the protection of the DRG from hypoxia and low pH stresses appears to be of equal importance.

CONFLICT OF INTEREST

The authors have nothing to disclose.

ACKNOWLEDGMENTS

This work was supported by the AO Foundation, AOSpine International and National Natural Science Foundation of China (NSFC, grants n. 81772333 and 51873069).

SUPPLEMENTARY MATERIALS

Supplementary video clips 1 and 2 can be found via https://doi.org/10.14245/ns.2040052.026.v1 and https://doi.org/10.14245/ns.2040052.026.v2.

Supplementary video clip 1. Calcium imaging of ND7/23 following preconditioning in 2% O_2 and pH 6.5 for 3 days. For ease of visualization, the videos were cropped to the last 7 seconds of spontaneous response and the first second following bradykinin addition. The overall recording lasted for 200 seconds with 100 seconds of spontaneous response and 100 seconds following bradykinin. The bradykinin-stimulated response in both soma and outgrowth can be visualized at the end of video (at the 8th second), while spontaneous response in cells preconditioned by 2% O_2 and pH 6.5 could be detected from 1 to 7 seconds. Scale bar equals 20 μm.

Supplementary video clip 2. Calcium imaging of ND7/23 following preconditioning in 20% O_2 and pH 7.4 for 3 days. For ease of visualization, the videos were cropped to the last 7 seconds of spontaneous response and the first second following bradykinin addition. The overall recording lasted for 200 seconds with 100 seconds of spontaneous response and 100 seconds following bradykinin. The bradykinin-stimulated response after 20% O_2 and pH 7.4 preconditioning can be visualized in both soma and outgrowth at the end of the video (at the 8th second) but seems to be weaker than cells preconditioned by 2% O_2 and pH 6.5. Spontaneous response in cells preconditioned in 20% O_2 and pH 7.4 could not be detected. Scale bar equals 20 μm.

ACKNOWLEDGMENTS

This work was supported by the AO Foundation, AOSpine International and National Natural Science Foundation of China (NSFC, grants n. 81772333 and 51873069).

REFERENCES

1. GBD 2016 Disease and Injury Incidence and Prevalence Collaborators. Global, regional, and national incidence, prevalence, and years lived with disability for 328 diseases and injuries for 195 countries, 1990-2016: a systematic analysis for the Global Burden of Disease Study 2016. Lancet 2017; 390:1211-59.
2. DePalma MJ, Ketchum JM, Saullo T. What is the source of chronic low back pain and does age play a role? Pain Med 2011;12:224-33.
3. Zhang YG, Guo TM, Guo X, et al. Clinical diagnosis for discogenic low back pain. Int J Biol Sci 2009;5:647-58.
4. Hangai M, Kaneoka K, Kuno S, et al. Factors associated with lumbar intervertebral disc degeneration in the elderly. Spine J 2008;8:732-40.
5. Kauppila LI. Atherosclerosis and disc degeneration/low-back pain--a systematic review. Eur J Vasc Endovasc Surg 2009; 37:661-70.
6. Kurunlahti M, Tervonen O, Vanharanta H, et al. Association of atherosclerosis with low back pain and the degree of disc degeneration. Spine (Phila Pa 1976) 1999;24:2080-4.
7. Holm S, Maroudas A, Urban JP, et al. Nutrition of the intervertebral disc: solute transport and metabolism. Connect Tissue Res 1981;8:101-19.
8. Walshe TE, D'Amore PA. The role of hypoxia in vascular injury and repair. Annu Rev Pathol 2008;3:615-43.
9. Wu WP, Jiang JM, Qu DB, et al. [Expression of hypoxia-inducible factor-1alpha and matrix metalloproteinase-2 in degenerative lumbar intervertebral disc]. Nan Fang Yi Ke Da Xue Xue Bao 2010;30:1152-5.
10. Richardson SM, Knowles R, Tyler J, et al. Expression of glucose transporters GLUT-1, GLUT-3, GLUT-9 and HIF-1alpha in normal and degenerate human intervertebral disc. Histochem Cell Biol 2008;129:503-11.
11. Keshari KR, Lotz JC, Link TM, et al. Lactic acid and proteoglycans as metabolic markers for discogenic back pain. Spine (Phila Pa 1976) 2008;33:312-7.
12. Nachemson A. Intradiscal measurements of pH in patients with lumbar rhizopathies. Acta Orthop Scand 1969;40:23-42.
13. Krames ES. The role of the dorsal root ganglion in the development of neuropathic pain. Pain Med 2014;15:1669-85.
14. Xiao WH, Bennett GJ. Persistent low-frequency spontaneous discharge in A-fiber and C-fiber primary afferent neurons during an inflammatory pain condition. Anesthesiology 2007;107:813-21.
15. Zhang JM, Song XJ, LaMotte RH. An in vitro study of ectopic discharge generation and adrenergic sensitivity in the intact, nerve-injured rat dorsal root ganglion. Pain 1997;72: 51-7.
16. Berta T, Qadri Y, Tan PH, et al. Targeting dorsal root ganglia and primary sensory neurons for the treatment of chronic pain. Expert Opin Ther Targets 2017;21:695-703.
17. Djouhri L, Koutsikou S, Fang X, et al. Spontaneous pain, both neuropathic and inflammatory, is related to frequency of spontaneous firing in intact C-fiber nociceptors. J Neurosci 2006;26:1281-92.
18. Kim YS, Anderson M, Park K, et al. Coupled activation of primary sensory neurons contributes to chronic pain. Neuron 2016;91:1085-96.
19. Rydevik BL, Myers RR, Powell HC. Pressure increase in the dorsal root ganglion following mechanical compression. Closed compartment syndrome in nerve roots. Spine (Phila Pa 1976) 1989;14:574-6.
20. Takebayashi T, Cavanaugh JM, Cüneyt Ozaktay A, et al. Effect of nucleus pulposus on the neural activity of dorsal root ganglion. Spine (Phila Pa 1976) 2001;26:940-5.
21. Parke WW, Whalen JL. The vascular pattern of the human dorsal root ganglion and its probable bearing on a compartment syndrome. Spine (Phila Pa 1976) 2002;27:347-52.
22. Kalichman MW, Myers RR. Transperineurial vessel constriction in an edematous neuropathy. J Neuropathol Exp Neurol 1991;50:408-18.
23. Myers RR, Powell HC. Galactose neuropathy: impact of chronic endoneurial edema on nerve blood flow. Ann Neurol 1984;16:587-94.
24. Myers RR, Murakami H, Powell HC. Reduced nerve blood flow in edematous neuropathies: a biomechanical mechanism. Microvasc Res 1986;32:145-51.
25. Song XJ, Hu SJ, Greenquist KW, et al. Mechanical and thermal hyperalgesia and ectopic neuronal discharge after chronic compression of dorsal root ganglia. J Neurophysiol 1999; 82:3347-58.
26. Lin XY, Yang J, Li HM, et al. Dorsal root ganglion compression as an animal model of sciatica and low back pain. Neu-

 https://doi.org/10.14245/ns.2040052.026

rosci Bull 2012;28:618-30.
27. Brisby H. Pathology and possible mechanisms of nervous system response to disc degeneration. J Bone Joint Surg Am 2006;88 Suppl 2:68-71.
28. Wood JN, Bevan SJ, Coote PR, et al. Novel cell lines display properties of nociceptive sensory neurons. Proc Biol Sci 1990;241:187-94.
29. Anderson M, Zheng Q, Dong X. Investigation of pain mechanisms by calcium imaging approaches. Neurosci Bull 2018; 34:194-9.
30. Wang F, Bélanger E, Paquet ME, et al. Probing pain pathways with light. Neuroscience 2016;338:248-71.
31. Gold MS, Gebhart GF. Nociceptor sensitization in pain pathogenesis. Nat Med 2010;16:1248-57.
32. Kleindienst T, Lohmann C. Simultaneous patch-clamping and calcium imaging in developing dendrites. Cold Spring Harb Protoc 2014;2014:324-8.
33. Nguyen C, Upadhyay H, Murphy M, et al. Simultaneous voltage and calcium imaging and optogenetic stimulation with high sensitivity and a wide field of view. Biomed Opt Express 2019;10:789-806.
34. Sasaki T, Takahashi N, Matsuki N, et al. Fast and accurate detection of action potentials from somatic calcium fluctuations. J Neurophysiol 2008;100:1668-76.
35. Vetter I, Lewis RJ. Characterization of endogenous calcium responses in neuronal cell lines. Biochem Pharmacol 2010; 79:908-20.
36. Fu M, Sun ZH, Zong M, et al. Deoxyschisandrin modulates synchronized Ca2+ oscillations and spontaneous synaptic transmission of cultured hippocampal neurons. Acta Pharmacol Sin 2008;29:891-8.
37. Francis M, Waldrup J, Qian X, et al. Automated analysis of dynamic Ca2+ signals in image sequences. J Vis Exp 2014; 51560.
38. Simpson AW. Fluorescent measurement of [Ca2+]c: basic practical considerations. Methods Mol Biol 2005;312:3-36.
39. Longair MH, Baker DA, Armstrong JD. Simple Neurite Tracer: open source software for reconstruction, visualization and analysis of neuronal processes. Bioinformatics 2011;27: 2453-4.
40. Light AR, Hughen RW, Zhang J, et al. Dorsal root ganglion neurons innervating skeletal muscle respond to physiological combinations of protons, ATP, and lactate mediated by ASIC, P2X, and TRPV1. J Neurophysiol 2008;100:1184-201.
41. Hjerling-Leffler J, Alqatari M, Ernfors P, et al. Emergence of functional sensory subtypes as defined by transient receptor potential channel expression. J Neurosci 2007;27:2435-43.
42. Suri P, Hunter DJ, Rainville J, et al. Quantitative assessment of abdominal aortic calcification and associations with lumbar intervertebral disc height loss: the Framingham Study. Spine J 2012;12:315-23.
43. International association for the study of pain. Task force on taxonomy. Classification of chronic pain. 2nd ed. Seattle (WA): IASP Press 1994.
44. Bennett GJ. What is spontaneous pain and who has it? J Pain 2012;13:921-9.
45. Dray A, Perkins M. Bradykinin and inflammatory pain. Trends Neurosci 1993;16:99-104.
46. Khan AN, Jacobsen HE, Khan J, et al. Inflammatory biomarkers of low back pain and disc degeneration: a review. Ann N Y Acad Sci 2017;1410:68-84.
47. Petho G, Reeh PW. Sensory and signaling mechanisms of bradykinin, eicosanoids, platelet-activating factor, and nitric oxide in peripheral nociceptors. Physiol Rev 2012;92:1699-775.
48. Paredes RM, Etzler JC, Watts LT, et al. Chemical calcium indicators. Methods 2008;46:143-51.
49. Charlton SJ, Vauquelin G. Elusive equilibrium: the challenge of interpreting receptor pharmacology using calcium assays. Br J Pharmacol 2010;161:1250-65.
50. Bonica JJ, Hoffman JF. The management of pain with special emphasis on the use of analgesic blocks in diagnosis, prognosis, and therapy. Anesth Analg 1954;34:57-8.
51. Bakker EW, Verhagen AP, Lucas C, et al. Daily spinal mechanical loading as a risk factor for acute non-specific low back pain: a case-control study using the 24-Hour Schedule. Eur Spine J 2007;16:107-13.
52. Steen KH, Steen AE, Reeh PW. A dominant role of acid pH in inflammatory excitation and sensitization of nociceptors in rat skin, in vitro. J Neurosci 1995;15(5 Pt 2):3982-9.
53. Latremoliere A, Woolf CJ. Central sensitization: a generator of pain hypersensitivity by central neural plasticity. J Pain 2009;10:895-926.
54. Ji RR, Berta T, Nedergaard M. Glia and pain: is chronic pain a gliopathy? Pain 2013;154 Suppl 1:S10-S28.
55. Ladewig T, Keller BU. Simultaneous patch-clamp recording and calcium imaging in a rhythmically active neuronal network in the brainstem slice preparation from mouse. Pflugers Arch 2000;440:322-32.
56. Bourinet E, Altier C, Hildebrand ME, et al. Calcium-permeable ion channels in pain signaling. Physiol Rev 2014;94:81-140.